Structural and Durability Investigation of the Vitreous Part of the System $(35\text{-}z)Na_2O\text{-}zFe_2O_3\text{-}5Al_2O_3\text{-}60P_2O_5$

Said Aqdim[1,2], El Hassan Sayouty[3] and Brahim Elouadi[1]*

[1]Laboratoire d'Elaboration, Analyse Chimique et Ingénierie des Matériaux (LEACIM),Université de la Rochelle, avenue Michel Crépeau, 17042 La Rochelle Cedex 01, France

[2]Laboratoire de Chimie Minérale, Département de Chimie, Université Hassan II Ain chock, Faculté des Sciences B.P. 5366 Maârif, km 8 route d'El-Jadida, Casablanca, Morocco

[3]Laboratoire de Physique de l'Etat Condensé Université Hassan II Ain chock, Faculté des Sciences – Casablanca B.P. 5366 Maârif, km 8 route d'El-Jadida, Casablanca, Morocco

Abstract

The glass compositions isolated within the system $(35\text{-}z)Na_2O\text{-}zFe_2O_3\text{-}5Al_2O_3\text{-}60P_2O_5$ ($5 \leq z \leq 20$), were found to belong to the domains of metaphosphate ($z = 5$) and oligo-phosphate ($5 < z \leq 20$) families. It was also found that less that 10 mol.% of iron present in the glass was under the reduced form Fe(II). The redox phenomenon of iron in these vitrified phosphates was attributed to the reduction conditions in the melts, created by the gas mixtures resulting from decomposition of the starting material $(NH_4)_2HPO_4$. Both X-ray crystallography and IR spectroscopy have confirmed the structural tendency change from the metaphosphate to the pyrophosphate structural units as the glass composition changes between the limits of $z = 5$ and $z = 20$. The chemical durability tends also to be improved in a significant manner as the ratio of Fe_2O_3 is increased. The analysis of the oxygen molar volume in this series of phosphate glasses, has allowed to conclude to the reinforcement of the covalent character of the chemical bond with increasing content of iron(III) oxide.

Introduction

Due to their poor chemical durability, phosphate glasses have rather limited technological applications despite their intensive investigation so far conducted by many researchers [1-19,22-24]. However several phosphate glasses with high aqueous corrosion resistance have been reported [3]. Their properties (low melting point, high thermal expansion coefficient, optical properties *etc.*) make these glasses serious potential candidates for many technological applications such as sealing materials, solid state electrolytes, laser hosts, *etc.*[2,3]. As a result of high chemical durability and low processing temperature, iron phosphate glasses have been considered as better candidates for the vitrifying of some types of nuclear wastes when compared with borosilicate glasses [4-7]. Various studies have shown that the chemical durability of phosphate glasses can be improved by the addition of various oxides such as Al_2O_3 and, especially, Fe_2O_3 [8-9]. Recently, the glass structure within the binary system Fe_2O_3-P_2O_5 has been investigated [10-16]. In addition, incorporation of Fe_2O_3 to the phosphate network was reported to lead to the breakdown of the P–O–P bonds and to the appearance of P–O–Fe units [15]. As expected, The effect of iron content on the structure of sodium-aluminium-iron phosphate glasses investigated by X-ray diffraction and IR spectroscopy, have shown a progressive evolution of the phosphate network for example from metaphosphate chains to the pyrophosphate structure with increasing iron ratio [4,5,16]. Therefore it has been suggested that the chemical durability of sodium-aluminium-iron phosphate glasses is attributed

*corresponding authors. E-mail: belouadi@univ-lr.fr

Printed in Kazakhstan

to the replacement of P–O–P bonds by Al–O–P and P–O–Fe bonds. The presence of the bands in higher concentrations, makes the glasses more hydration resistant [18-21]. The potentiometric measurements carried out on aqueous solutions of iron phosphate glasses, have shown that the ratio [Fe(II)]/[Fe(II) + Fe(III)] varies between 6 and 8 for the investigated materials with increasing iron content [18,21,22,24-26]. The speciation of iron in these glasses is controlled by the following reversible reaction:

$$4Fe^{2+}_{melt} + O_{2\ melt\ atm} \Leftrightarrow 4\ Fe^{3+}_{melt} + 2O^{2-}_{melt}$$

It has also been mentioned that the redox phenomenon of iron tends to play an important role in the increasing chemical durability of the corresponding glasses [18,21]. The purpose of the present work is to investigate the mixed effects of alkaline aluminium and iron cation on the structure and the durability of selected phosphate glasses in the system (35-*z*)Na_2O-*z*Fe_2O_3-5Al_2O_3-60P_2O_5.

Experimental

Glasses of different compositions have been prepared from the appropriate mixture of the starting compounds Na_2CO_3, Al_2O_3, Fe_2O_3 and $(NH_4)_2HPO_4$. The weighted mixture of about 10 g were thoroughly in an agate mortar before to be submitted to moderate heat treatments between 300°C and 500°C in order to achieve a preparation before the glass preparation. The melt was achieved for about 15 nm at 1070±10°C. The batch quenched at room temperature, has then allowed to isolate glass samples with approximate sizes of 5-10 nm diameter and 1-3 mm thickness. The vitreous state was first evidenced from the shiny aspect and then confirmed from XRD patterns.

The chemical durability of these vitrified phosphates has been evaluated from the weight loss of samples having a size of about 0.9×0.9×0.3 cm^3. Prior to any aqueous treatment, the samples for tests were polished to 400 grit finish with SiC paper, cleaned with acetone and immersed for 20 continuous days in glass flasks containing 100 ml of distilled water at 90°C. The density of each glass composition was measured using the helium pycnometry method. Iron redox ratio [Fe(II)]/[Fe(II) + Fe(III)] was determined by potentiometric method which allowed to determine both iron Fe^{2+} and iron Fe^{3+} concentration after the chemical neutralization with dichromate solution. The analysed glass solution was obtained after a complete digestion of the appropriate sample in concentrated H_2SO_4 solution. Details of the potentiometric method were given elsewhere [26]. The experimental error made during the determination of the ratio [Fe(II)]/[Fe(II) + Fe(III)] was found to be about ±2 (Table 1). All infrared (IR) spectra for the glasses were recorded within the range 400-1600 cm^{-1}, on KBr based pellets (2 mg glass in about 100 mg KBr) using mX-1 and NIC-3600 FTIR spectrometers. The chemical compositions of the batches, given in terms of the starting mixture of oxides, are recapitulated in Table 1. Indeed, as evidenced from the data of Table 1, the investigated glasses can be classified as quaternary glasses within the system [(35-*z*)Na_2O-*z*Fe_2O_3-5Al_2O_3-60P_2O_5]. Since the existence of iron(II) has been evidenced in all elaborated samples, both by potentiometric and Mössbauer results [25], part of iron ions in the glass have been found to be Fe^{2+} (Table1, § 32 here below), the most rigorous system for the localization of the glasses would be the quinary diagram [(35-*z*) Na_2O-(*z*-*t*)Fe_2O_3-*t*$(FeO)_2$-5Al_2O_3-60P_2O_5].

Table 1

Some characteristics of the quaternary glasses (35-z)Na_2O zFe_2O_3-5Al_2O_3-60P_2O_5
(see Figure 1, for the positions of samples G_5^{60}-G_{20}^{60} within the appropriate ternary diagram)

Glass Sample	Starting oxide mixtures, mol.%				$[Fe^{2+}]/[(Fe^{3+} + Fe^{2+})]$	[O/P] ratio	D_R*, g·cm^{-2}·min^{-1}
	Na_2O	Fe_2O_3	Al_2O_3	P_2O_5			
G_5^{60}	30	5	5	60	6±2	3	(1.2±0.2)×10^{-6}
G_{10}^{60}	25	10	5	60	9±2	3.08	(2.5±0.2)×10^{-7}
G_{15}^{60}	20	15	5	60	7±2	3.17	(1.2±0.2)×10^{-7}
G_{20}^{60}	15	20	5	60	8±2	3.25	(9±0.2)×10^{-9}

*(D_R) represents the weigh loss after 20 days of aqueous attack at 90°C, in distilled H_2O.

As the relative concentration of iron(II) is rather limited to less than 10%, it was considered here for a better and vivid presentation (Fig. 1) to consider only the basic oxides given in Table 1. As a matter of fact, the so low ratio of iron(II) in the vitrified compositions is not expected to have significant effect on the structural change of glass network and properties. Indeed, the ternary diagram given in Fig. 1, corresponds to one section of the original quaternary system, at a fixed molar fraction of 60 mol.% P_2O_5. Therefore, the glass materials can be expressed in terms of the basic constituents of the pseudo-ternary diagram: [$2Na_2O{\cdot}3P_2O_5$]-($2Fe_2O_3{\cdot}3P_2O_5$)-($2Al_2O_3{\cdot}3P_2O_5$)], as reported in Table 2.

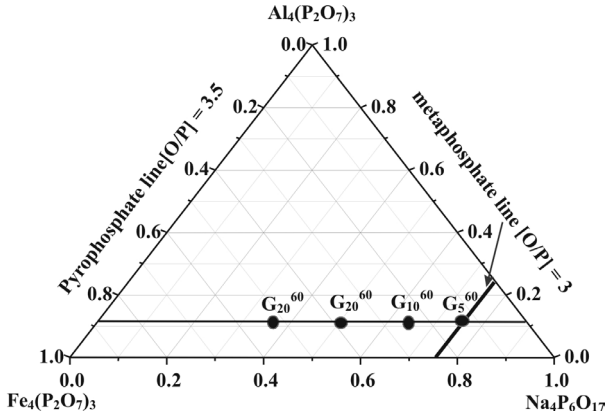

Fig. 1. Localization of the investigated glass compositions G_5^{60}, G_{10}^{60}, G_{15}^{60} and G_{20}^{60} within the ternary diagram ($2Na_2O{\cdot}3P_2O_5$)-($2Al_2O_3{\cdot}3P_2O_5$)-($2Fe_2O_3{\cdot}3P_2O_5$). Table 1 gives the corresponding compositions within the quaternary system Na_2O-Fe_2O_3-Al_2O_3-P_2O_5.

Results and Discussions

Structural Analysis

X-Ray Crystallography Results

X-ray crystallography has confirmed the vitreous character of all the investigated glass samples. Indeed, the recorded X-ray diffraction (XRD) patterns were found to be typical of amorphous substances. As expected, its is also worth to notice that the sintering of the samples G_5^{60} and G_{15}^{60} at 540 and 630°C respectively has resulted in their crystallization as evidenced from their new XRD-patterns given in Fig. 2. The analysis of the latter patterns allows the following conclusions:

- The sample G_5^{60} tends to crystallize in a mixture of networks close to those of metaphosphates of Na, Al, Fe and related mixed oxides. As expected, due to its position in the phase diagram of Fig. 1, such glass of composition G_5^{60} belongs to the metaphosphate line. The crystallization is then compatible with these phosphate family characterized by the ratio [O/P] = 3.
- The sample G_{15}^{60} (Fig. 1) belongs to the oligophosphate domain (with $3 < [O/P] < 3.5$) is expected to contain mixture of meta- and pyrophosphate networks related to those of sodium, aluminium and iron. As a result of their positions in the ternary diagram, the crystallisation of all samples G_5^{60}, G_{10}^{60}, G_{15}^{60}, and G_{20}^{60} is therefore expected to give rise to crystalline precipitates of mono and diphosphates of one or mixed cations Na^+, Fe^{2+}, Al^{3+} and/or Fe^{3+}.

The crystallization process has allowed us to approach the glass structure of our vitreous systems on the basis of the theory of crystallites [27]. This model has been confirmed by IR vibration spectroscopy. Indeed the local structures of glass and the crystals of the same composition are reputed to be identical. This is the result that our present X-ray crystallography investigations have confirmed.

Infrared Vibration Spectroscopy Study

The recorded IR spectra of the glass series (35-*z*) Na_2O-*z*Fe_2O_3-5Al_2O_3-60P_2O_5 ($5 \le z \le 20$), are shown

Table 2
Glass compositions expressed in terms of ternary and quaternary systems

Glass sample	Chemical composition	Glass compositions inside the ternary diagram
G_5^{60}	$30Na_2O{\cdot}5Fe_2O_3{\cdot}5Al_2O_3{\cdot}60P_2O_5$	$0.75(2Na_2O{\cdot}3P_2O_5){\cdot}0.125(2Al_2O_3{\cdot}3P_2O_5){\cdot}0.125(2Fe_2O_3{\cdot}3P_2O_5)$
G_{10}^{60}	$25Na_2O{\cdot}10Fe_2O_3{\cdot}5Al_2O_3{\cdot}60P_2O_5$	$0.625(2Na_2O{\cdot}3P_2O_5){\cdot}0.125(2Al_2O_3{\cdot}3P_2O_5){\cdot}0.25(2Fe_2O_3{\cdot}3P_2O_5)$
G_{15}^{60}	$20Na_2O{\cdot}15Fe_2O_3{\cdot}5Al_2O_3{\cdot}60P_2O_5$	$0.50(2Na_2O{\cdot}3P_2O_5){\cdot}0.125(2Al_2O_3{\cdot}3P_2O_5){\cdot}0.375(2Fe_2O_3{\cdot}3P_2O_5)$
G_{20}^{60}	$15Na_2O{\cdot}20Fe_2O_3{\cdot}5Al_2O_3{\cdot}60P_2O_5$	$0.375(2Na_2O{\cdot}3P_2O_5){\cdot}0.125(2Al_2O_3{\cdot}3P_2O_5){\cdot}0.5(2Fe_2O_3{\cdot}3P_2O_5)$

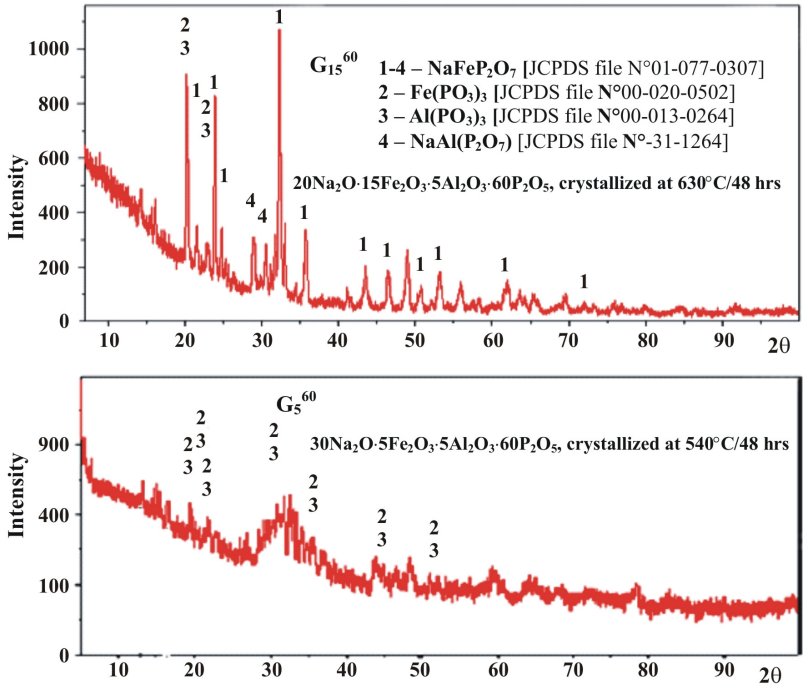

Fig. 2. XRD patterns, for the glass sample G_5^{60} and G_{15}^{60} after a heat treatment of 48 hrs under air atmosphere at 540°C and 630°C respectively.

in Fig. 3. The assignments of the vibration bands are given in Table 3. The spectrum of the vitreous sample G_5^{60}, $30Na_2O$-$5Fe_2O_3$-$5Al_2O_3$-$60P_2O_5$, is found to be compatible with the metaphosphate glass structure [2,10,16,28,29]. The band at 750 cm^{-1} was assigned to the symmetric stretching ν_{sym}(P–O–P) of the phosphorus tetrahedral bridge while the band at 910 cm^{-1} is assigned to the asymmetric stretching of the same bride, ν_{asym}(P–O–P). Additionally a weak band at about 770-785cm^{-1} in all probability due to Al–O stretching in AlO_4 groups is also located in the spectrum of these glasses [20, 21]. In the other hand in the region 500-560 cm^{-1}, the band due to FeO_6 groups is also present; it is assign to skeleton deformation (δ_{ske}) [26].

The band at 1290 cm^{-1} is attributed to the asymmetric stretching of two non bridging oxygens, $\nu_{asym}(PO_2)$ [2,16]. The band at 1060 cm^{-1} was assigned to $\nu_{sym}(PO_2)$. For higher values of z, the band at 1084 cm^{-1} was attributed to the pyrophosphate groups.

Figure 3 shows that with increasing value of z, the glass structure tends to change from the metaphosphate to the pyrophosphate region. As can be deduced from the assignment of the vibrational modes (Fig. 3 & Table 3), such composition change from the metaphosphate (G_5^{60}) to the oligophosphate family (G_{10}^{60}, G_{15}^{60}, G_{20}^{60}) can be followed by IR spectroscopy. As a matter of fact, with increasing values of z, the intensity of the characteristic bands of the metaphosphate glass tend to decrease while the typical bands of the pyrophosphate groups tend to remain and to dominate the spectrum as in the composition G_{20}^{60} with the ratio [O/P] ≈ 3.2. Indeed this ultimate composition does not reach the pyrophosphate line ($2Al_2O_3·3P_2O_5$-$2Fe_2O_3·3P_2O_5$) cor-

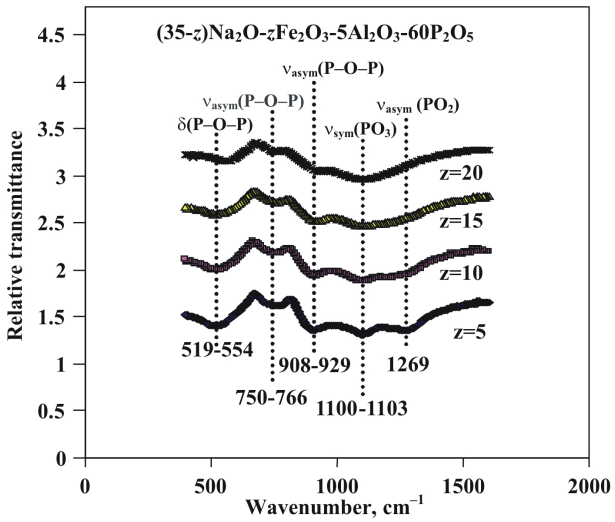

Fig. 3. The IR spectra of the series glasses (35-z)Na_2O-zFe_2O_3-$5Al_2O_3$-$60P_2O_5$.

Table 3

Assignment of the vibration modes of the IR spectra recorded for the glass system (35-*z*)Na_2O-*z*Fe_2O_3-5Al_2O_3-60P_2O_5

Sample G_5^{60} (z = 5, [O/P] = 3)		Sample G_{10}^{60} (z = 10, [O/P] = 3.08)		Sample G_{15}^{60} (z = 15, [O/P] = 3.17)		Sample G_{20}^{60} (z = 20, [O/P] = 3.25)		Literature data	
Frequency, cm^{-1}	**Mode assignment**	**Frequency, cm^{-1}**	**Mode assignment**	**Frequency, cm^{-1}**	**Mode assignment**	**Frequency, cm^{-1}**	**Mode assignment**	**Frequency, cm^{-1}**	**Refs.**
520 (VS)	δ_{ske}, FeO_6 Units	519(VS)	δ_{ske}, FeO_6 Units	511(S)	δ_{ske}, FeO_6 Units	554 (S)	δ_{ske}, FeO_6 Units	420 ; 440 490-560 508-574	32 33 23, 35, 36
766 (S)	ν_{sym} (P–O–P) AlO_4 Units	750 (S)	ν_{sym} (P–O–P) AlO_4 Units	750 (M)	ν_{sym} (P–O–P) AlO_4 Units	751 (M-w)	ν_{sym} (P–O–P) AlO_4 Units	706-746 730-770 770-800	32 33 8,23,35,37
929 (VS)	ν_{asym} (P–O–P)	908 (S)	ν_{asym} (P–O–P)	908 (S)	ν_{asym} (P–O–P)	908 (S)	ν_{asym} (P–O–P)	916-990 923 990	33 23 33
1060 (S)	$\nu_{sym}(PO_2)$	1060 (S)	$\nu_{sym}(PO_2)$					1080 1106 1120	23, 37 32 33
				1070 (S)	$\nu_{sym}(PO_3)$/ $\nu_{asym}(PO_3)$	1084 (S)	$\nu_{sym}(PO_3)$/ $\nu_{asym}(PO_3)$	990-1146 1100-1190 1280 1330	32 34 8 23, 37
1269 (S)	$\nu_{asym}(PO_2)$	1260(W)	$\nu_{asym}(PO_2)$	–		–		1200-1240 1200-1250 1260-1290	34 33 32
Metaphosphate structural type		Oligophosphate structural type		Oligophosphate structural type		Pyrophosphate dominant structure			

responding to the ratio [O/P] = 3.5. However, the dominant structure of pyrophosphate network resulting from the increasing ratio of iron(III) oxide, is evidenced by IR and XDR techniques:

- IR results show that the pyrophosphate characteristic band, $\nu_{sym}(PO_3)$ tend to dominate the spectrum (Fig. 3) as it becomes wider with higher intensity;
- RXD patterns (Fig. 2) of crystallized G_5^{60} sample, are exclusively similar to the metaphosphate XRD patterns of $Al(PO_3)_3$ and $Fe(PO_3)_3$, taken from their respective JCPDS files N°00-013-0264 and 00-020-0502;
- XRD patterns of G_{15}^{60} seem to be more compatible with pyrophosphates units since these patterns are similar to those of $NaFeP_2O_7$ (JCPDS file N°01-077-0307) and $AlFeP_2O_7$ (JCPDS file N°31-1264).

Analysis of the Oxygen Molar Volume

Density measurements have allowed to follow the change of the molar volume versus composition along the system (35-*z*)Na_2O-*z*Fe_2O_3-5Al_2O_3-60P_2O_5. As can be deduced from the plots of Fig. 4, density (more precisely the specific mass) is increasing with increasing ratio of Fe_2O_3. The oxygen molar volume and the oxygen anion radius in the glass were determined from *eq.* 1 and *eq.* 2, respectively:

$$V_{OM} = M/[\rho N_A \cdot N_O] \quad (1)$$

$$r_{cal}(O^{2-}) = \frac{\sqrt[3]{V_{OM}}}{2} \quad (2)$$

with M = molar mass; ρ = density; N_A = Avogadro number; N_O = number of oxygen atoms contained in the molar formula.

A fine analysis of the data given in Table 4, shows that the molar volume is decreasing versus increasing iron(III) oxide content. The value of the relative radius of oxygen anion $r_{cal}(O^{2-})$, calculated from the molar volume (*eq.* 2) is also decreasing from $r_{cal}(O^{2-})$ = 1.43 Å (for z = 5) to 1.37 Å (for z = 20). It is also worth to notice that the $r_{cal}(O^{2-})$ diminishes as the glass composition tends to change from the

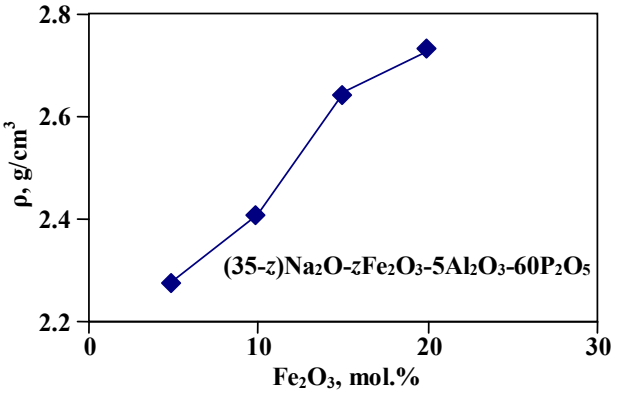

Fig. 4. Variation of the Density (ρ) versus mol.% Fe_2O_3 along the glass series (35-*z*)Na_2O-*z*Fe_2O_3-5Al_2O_3-60P_2O_5.

metaphosphate domain (G_1^{60}) to the pyrophosphate line ($2Al_2O_3{\cdot}3P_2O_5$-$2Fe_2O_3{\cdot}3P_2O_5$) according to the sequence $G_5^{60} \rightarrow G_{10}^{60} \rightarrow G_{15}^{60} \rightarrow G_{20}^{60}$. Such decrease of $r_{cal}(O^{2-})$ which evidences the shortening of the inter-atomic distances has been interpreted as a strengthening of the chemical bond with the increase of its covalent character in the investigated glasses.

Iron(II)/Iron(III) Redox Phenomenon

Like all transition elements, iron is reputed to have at least two oxidation degrees under normal atmospheric conditions. Therefore, as expected the starting iron (III) oxide has been reduced during the elaboration of the title phosphate glasses. Indeed the batch melting is realised in a rather reduced atmosphere which is created by the decomposition of the starting compound $(NH_4)_2HPO_4$ witch gives rise at high temperatures, to a gas mixture of the type ($NH_{3(g)}$ + $H_{2(g)}$ + $H_2O_{(g)}$) for example. The potentiometric measurements have confirmed the coexistence of the two oxidation degrees (Fe^{2+} and Fe^{3+}) in all synthesized glasses (G_5^{60}, G_{10}^{60}, G_{15}^{60} and G_{20}^{60}). Equivalent redox phenomena with iron and other transition element phosphate glasses have been reported by various authors [8,18,24,36-48]. It is also worth to notice that the ratio $[Fe^{2+}]/[Fe^{3+} + Fe^{2+}]$ tends to be invariant in all elaborated glasses (Table 1). This could be probably explained by the fact that the same elaboration procedure was used to prepare all samples. As a consequence, the same reduction power of the emanating gas mixtures ($NH_{3(g)}$ + $H_{2(g)}$ + $H_2O_{(g)}$) is expected to result in the same mol.% of reduction of starting iron oxide (Fe_2O_3) in the melt. Therefore, the same reduction conditions are expected to produce the same values of the ratio $[Fe^{2+}]/[Fe^{3+} + Fe^{2+}]$ which was estimated here to be of the approximate order of 7-8%, as evidenced from the experimental results given in Fig. 5.

Analysis of the Chemical Durability of the Glass Series (35-z)Na_2O-zFe_2O_3-5Al_2O_3-60P_2O_5

The chemical durability of this series of glasses was approached using the measurement of the dissolution (D_R) rate which was defined as the weight loss of the glass expressed in terms of $g{\cdot}cm^{-2}{\cdot}min^{-1}$. The values of ($D_R$) given in Table 1 show a dissolu-

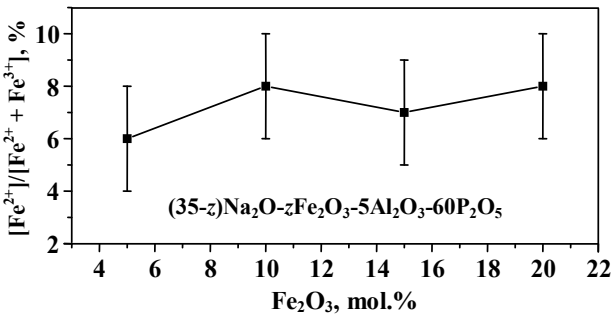

Fig. 5.Variation of the ratio $[Fe^{2+}]/[Fe^{2+} + Fe^{3+}]$ versus mol.% Fe_2O_3 along the system (35-*z*)Na_2O-*z*Fe_2O_3-5Al_2O_3-60P_2O_5 (Table1).

Table 4
Density and related molar data of the system (35-*z*)Na_2O-zFe_2O_3-5Al_2O_3-60P_2O_5

Sample	Molar formula	Molar mass, g·mol^{-1}	Density ρ, g/cm^3	Molar volume (Å^3) $V_{OM} = M/[\rho N_A{\cdot}N_O]$*	Calculated oxygen radius (Å) $r_{cal}(O^{2-})$
G_5^{60} (z = 5)	$30Na_2O{\cdot}5Fe_2O_3{\cdot}5Al_2O_3{\cdot}60P_2O_5$	11684.7	2.28	23.6	1.43
G_{10}^{60} (z = 10)	$25Na_2O{\cdot}10Fe_2O_3{\cdot}5Al_2O_3{\cdot}60P_2O_5$	12173.1	2.41	22.7	1.42
G_{15}^{60} (z = 15)	$20Na_2O{\cdot}15Fe_2O_3{\cdot}5Al_2O_3{\cdot}60P_2O_5$	12661.5	2.65	20.9	1.38
G_{20}^{60} (z = 20)	$15Na_2O{\cdot}20Fe_2O_3{\cdot}5Al_2O_3{\cdot}60P_2O_5$	13149.9	2.73	20.5	1.37

*M = molar mass; ρ = density; N_A = Avogadro number; N_O = number of oxygen atoms in the molar formula

tion decrease (versus mol.% Fe_2O_3). The plots given in Figure 6, are typical results obtained for samples after their immersion in 100 ml of distilled water, heated at 90°C during 20 consecutive days. It is also worth to compare the (D_R) data of the present work to other values reported in the literature [15,24,25]. Indeed the glass sample G_{20}^{60} (20 mol.% Fe_2O_3) was found to have equivalent durability value of the order of that found for window glass which is also about 50 times smaller than the dissolution rate of glass (27BaO·45B_2O_3·18Al_2O_3·10Fe_2O_3) BABAL. It is also worth to mention that the borate BABAL glass has been considered as alternative material for the immobilization of nuclear waste substances [15,24]. In addition, the value (1.4×10^{-5}-1.3×10^{-9} g·cm^{-2}·min^{-1}) of (D_R) reported by Reis *et al.* [24] for the glass system [(40-*x*)ZnO-*x*Fe_2O_3-60P_2O_5]; is very close to the one we found in the present study: 1.2×10^{-6}-9×10^{-9} (Table1).

Correlation Between Chemical Bonds, Structure and the Chemical Durability

Both XRD and IR techniques have confirmed the structural evolution of the glass network along the series (35-*z*)Na_2O-zFe_2O_3-5Al_2O_3-60P_2O_5, when the compositions is changed from the metaphosphate (G_5^{60}) towards the pyrophosphate line with [O/P] = 3.5 (Fig. 1). The diminishing of the oxygen molar volume (Table 4) versus *z*, tends to confirm the increase of the covalent character of the chemical bond with increasing Fe_2O_3 content in the glass. The intensification of this covalent character may probably explain the chemical strength of glass network which becomes more resistant to the chemical attack in an aggressive aqueous medium at 90°C.

In addition, some authors have attributed the elevated chemical durability of our equivalent quaternary iron phosphate glasses (Table 1), to the increasing number of Fe–O–P bonds in the vitreous network [19,22]. Such bonds are expected to be more water resistant than the P–O–P one, which constitute the majority in the samples with low iron concentration. Indeed as the glass series progresses from the metaphosphate point G_5^{60} towards G_{20}^{60} with a composition closer to pyrophosphates, the number of links P–O–P is decreasing while the number of Fe–O–P bonds is significantly increasing. Due to the low electro-negativity value of iron, the chemical bond Fe–O is expected to be of higher ionic character. However, the nature of the chemical bonds of both iron(II) and iron(III) in the present glasses have not yet been deeply investigated.

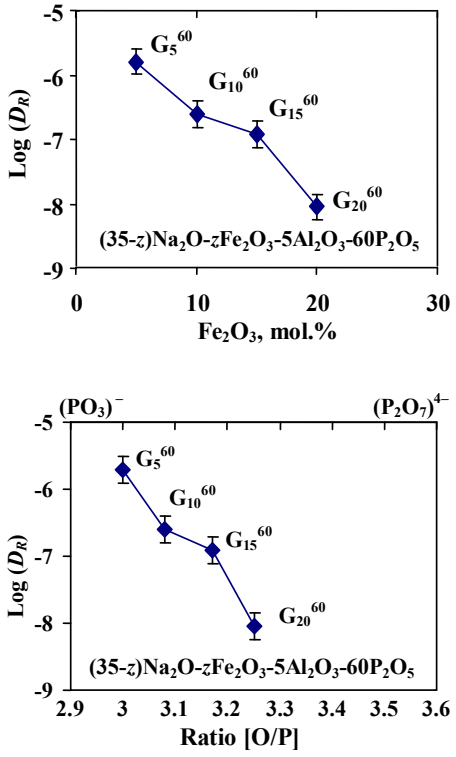

Fig. 6. Dissolution rates (D_R) of the glass series (35-*z*)Na_2O-zFe_2O_3-5Al_2O_3-60P_2O_5 versus: a) Fe_2O_3 (mol.%); b) ratio [O/P]. The chemical compositions are given in Table1.

Conclusions

The structure and the chemical durability of sodium aluminium iron phosphate glasse series (35-*z*) Na_2O-zFe_2O_3-5Al_2O_3-60P_2O_5, have been investigated using various techniques such as IR, XRD, *etc*. The vitreous pyrophosphate structure was found to be reinforced with increasing content of Fe_2O_3 in the materials. It was also confirmed that the dissolution rates (D_R) of the analysed compounds is comparable to the values of borosilicate glasses and 50 times smaller than of BABAL glasses which have been considered as alternative materials for the immobilization of nuclear waste substances. This is a very important and encouraging result because among all potential applications, our glasses appear as serious candidates for the nuclear waste management. It was also found that the covalent character of the chemical bond is enhanced with increasing ratio of iron oxide in the elaborated glasses. Furthermore, the improved chemical durability with raising iron content is compatible with the increase of corrosion resistant Fe–O–P bonds in all vitrified samples.

References

1. R.K. Brow, C.M. Arens, X. Yu and D.E. Day; Phys. Chem. Glasses 35 (1994)132.
2. M. Ouchetto; Thèse de Doctorat d'Etat es Sciences, Faculty of Sciences Rabat, Morocco (1993).
3. R.K Brow; J. Non-Cryst. Solids 263&264 (2000) 1.
4. A. Mogus-Milankovic, B. Pivac, K. Furic, and D. E. Day; Phys. Chem. Glasses 38 (1997) 74.
5. A. Mogus-Milankovic, M. Rajic, A. Drasner, R. Trojko and D.E. Day; Phys. Chem.Glasses 39 (1998) 70.
6. D.E. Day, Z. Wu, C.S. Ray, P. Hrma; J. Non-Cryst. Solids 241 (1998)1.
7. B.C. Sales, L.A. Boatner; Science 226(1984) 45.
8. X. Fang, C.S. Ray, A. Mogus-Milankovic, and D.E. Day; J. Non-Cryst. Solids 283 (2001) 162.
9. X. Fang, C.S. Ray, G.K. Marasinghe, and D.E. Day; J. Non-Cryst. Solids. 263&264 (2000) 293.
10. A. Mogus-Milankovic, A. Gajovic, A. Santic, and D.E. Day; J. Non-Cryst. Solids. 289 (2001) 204.
11. M. Karabulut, G.K. Marasinghe, C.S. Ray, G.D. Waddill, D.E. Day, Y.S. Bady, L. Saboungi, S. Shastri, D. Haeffner, J. Appl. Phys. 87 (2000) 2185.
12. M. Karabulut, G.K. Marasinghe, C.S. Ray. D.E. Day, O. Ozturk, G.D Wadill; J. Non-Cryst. Solids 249 (1999) 105.
13. C.H. Booth, P.G. Allen, J.J. Bucher, N.M. Edelstein, D.K. Shuh, G.K. Marasinghe, M. Karabulut, C.S. Ray, D.E. Day; J. Mater. Res. 14 (1999) 2628.
14. M. Karabulut, G.K. Marasinghe, C.SRay, G.D. Waddill, D.E Day, Y.S. Bady, L. Saboungi, S. Shastri, D. Haeffner, J. Appl. Phys. 87 (2000) 2185.
15. C.S. Ray, X. Fang, M. Karabulut, G.K. Marasinghe, D.E. Day; J. Non Cryst. Solids 249 (1999) 1.
16. S. Aqdim, Diplôme d'Etudes Supérieures de 3ème Cycle de Spécialité; University Mohammed-5, Faculty of Science (1990) Rabat, Maroc.
17. X. Fang, C.S. Ray, G.K. Marasinghe and D.E. Day; J. Non-Cryst. Solids 263 & 264 (2000) 293.
18. B.C. Sales, M.M. Abraham, J.B. Bates and L.A. Boatner; J. Non-Cryst. Solids 71 (1985) 103.
19. J.S. Brooks, G.L. Williams and D.W. Allen; Phys. Chem. Glasses 33 (1992) 171.
20. A. Veerabhadra Rao, C. Laxmikanth, B. Appa Rao and N. Veeraiah; J. Phys. Chem. Solids 67(2006) 2478-2488.
21. M. Srinivasa Reddy, G. Naga Raju, G. Nagarjuna, N. Veeraiah; Journal of alloys and Compounds 438 (2007) 41-51.
22. X. Yu, D.E. Day, G.J. Long and R. K. Brow; J. Non-Cryst. Solids 215 (1997) 21.
23. B. Kumar and S. Lin; J. Am. Ceram. Soc. 74 (1991) 226.
24. S.T. Reis , M. Karabulut and D.E. Day; J. Non-Cryst. Solids 292 (2001) 150.
25. S. Aqdim, Thèse de Doctorat d'Etat ès Sciences, University Hassan-2, Faculty of Sciences, Casablanca, Morocco (2007).
26. A. Veerabhadra Rao, C. Laxmikanth, B. Appa Rao and N. Veeraiah; J Phys. Chem. Solids 67 (2006) 2263-2274.
27. P.I.K. Onorato, D. R. Uhlmann and R.W. Hopper; Journal of Non-Crystalline Solids 41 (1980) 189-200.
28. D.R. Tallant, C. Nelson; Phys. Chem. Glasses 27 (1986).75.
29. N.B. Nelson and G.J. Exarhos; J. Chem. Phys. 71 (1979) 2739.
30. C. Garrigou-Lagrange, M. Ouchetto and B. Elouadi; Can; J. Chem. 63 (1985) 1436.
31. M. Ouchetto, B. Elouadi and S. Parke; Phys. Chem. Glasses 32[2] (1991) 43.
32. D. Boudlich, L. Bih, M.E. Archidi, M. Haddad, A. Yacoubi, A. Nadiri and B. Elouadi; J. Am. Ceram. Soc. 85[3] (2002) 623.
33. M. Karabulut, G.K. Marasinghe, P.G. Allen, C.H. Booth, M. Grimsditch; J. Mater. Res. 15 (2000) 1972.
34. B. Samuneva, P. Tzvetkova, I. Gugov, V. Dimitrov; J. Mater. Sci. Lett. 1 5(1996)21.
35. A.M. Efimov; J. Non-Cryst. Solids 209 (1997) 209.
36. R.K. Brow, R.J. Kirkpatrick and G.L. Turner; J. Am. Ceram. Soc. 76 (1993) 919.
37. H. Doweidar, Y.M, Moustafa, K. El-Egili, I. Abbas; Vibrational Spectroscopy 37 (2005) 91.
38. M. Karabulut, E. Melnik, R. Stefan, G. K. Marasinghe, C.S. Ray, C. R. Kurkjian, D.E. Day; J. Non-Cryst. Solids 288 (2001) 8.
39. A. Mogus-Milankovic, A. Santic, A. Gajovic, D.E. Day; J. Non-Cryst. Solids 296 (2001) 57.
40. L. Bih, L. Abbas, A. Nadiri, H. Khemakhem and

B. Elouadi; J. Mol. Struct. (under press; 2007).
41. L. Armelao, M. Bettinelli, G.A. Rizzi, and U. Russo; J. Mater. Chem. 1 (1991) 805.
42. Punita Singh, S.S. Das and S.A. Agnihotry; J. Non-Cryst. Solids 315 (2005) 3730.
43. A. Mogus-Milankovic, A. Santic, S.T. Reis , K. Furic, and D.E. Day; J. Non-Cryst. Solids 351 (2005) 3246.
44. A. Mogus-Milankovic, A. Santic, S.T. Reis , K. Furic, and D.E. Day; J. Non-Cryst. Solids 342 (2004) 97.
45. K. Hirao, T. Komatsu and N. Soga; J. Non-Cryst. Solids 40 (1980) 315.
46. M-H. Chopinet, D. Luzarazu, C. Rocanière; C. R. Acad. Sci. Chimie (Paris) 5 (2002) 939.
47. N. Amraoui, Diplôme d'Etudes Supérieures de 3-ème Cycle, University Mohammed-V, Faculty of Sciences, Rabat Morocco (1990).
48. G.S.M. Partiti; J. Non Cryst. Solids 304 (2002) 188.

Received 20 November 2007